

This is the author's final, peer-reviewed manuscript as accepted for publication (AAM). The version presented here may differ from the published version, or version of record, available through the publisher's website. This version does not track changes, errata, or withdrawals on the publisher's site.

2022 CEOS International Thermal Infrared Radiometer Comparison. Part I: Laboratory Comparison of Radiometers and Blackbodies

Yoshiro Yamada, Subrena Harris, Michael Hayes, Rob Simpson, Werenfrid Wimmer, Raymond Holmes, Tim Nightingale, Arrow Lee, Nis Jepsen, Nicole Morgan, Frank-M. Göttsche, Raquel Niclòs, Martín Perelló, Craig Donlon, Nigel Fox

Published version information

Citation: Yamada, Y., and Coauthors, 2024: 2022 CEOS International Thermal Infrared Radiometer Comparison. Part I: Laboratory Comparison of Radiometers and Blackbodies. *J. Atmos. Oceanic Technol.*, 41, 295–307,

DOI: <https://doi.org/10.1175/JTECH-D-23-0059.1>.

This is the accepted version of the following article: Yamada, Y., and Coauthors, 2024: 2022 CEOS International Thermal Infrared Radiometer Comparison. Part I: Laboratory Comparison of Radiometers and Blackbodies. *J. Atmos. Oceanic Technol.*, 41, 295–307, which has been published in final form at https://journals.ametsoc.org/view/journals/atot/41/3/JTECH-D-23-0059.1.xml?tab_body=pdf.

This version is made available in accordance with publisher policies and with the licensing statement contained in the manuscript, under a [CC-BY licence](#) with permission from the authors. Please cite only the published version using the reference above. This is the citation assigned by the publisher at publication. Please check the publisher's website for any updates.

This item was retrieved from **ePubs**, the Open Access archive of the Science and Technology Facilities Council, UK. Please contact epublications@stfc.ac.uk or go to <http://epubs.stfc.ac.uk/> for further information and policies.

19

ABSTRACT

20 An international comparison of field deployed radiometers for sea surface skin
21 temperature (SST_{skin}) retrieval was conducted in June 2022. The campaign comprised a
22 laboratory and a field comparison. In the laboratory part the radiometers were compared
23 against reference standard blackbodies, while the same was done with the blackbodies used
24 for the calibration of the radiometers against a transfer standard radiometer. Reference values
25 were provided by the National Physical Laboratory (NPL), traceable to the primary standard
26 on the International Temperature Scale of 1990. This was followed by the field comparison at
27 a seaside pier on the south coast of England, where the radiometers were compared against
28 each other while viewing the closely adjacent surface of the sea. This paper reports the results
29 of the laboratory comparison of radiometers and blackbodies.

30 For the blackbody comparison, the brightness temperature of the blackbody reported by
31 the participants agreed with the reference value measured by the NPL transfer standard
32 radiometer within the uncertainties for all temperatures and for all blackbodies. For the
33 radiometer comparison, the temperature range of most interest from the SST_{skin} retrieval point
34 of view is 10 °C to 30 °C, and in this temperature range, and up to the maximum comparison
35 temperature of 50 °C, all participants' reported results were in agreement with the reference.
36 On the other hand, below 0 °C the reported values showed divergence from the reference and
37 the differences exceeded the uncertainties. The divergence shows there is room for
38 improvement in uncertainty estimation at lower temperatures, although it will have limited
39 implication in the SST_{skin} retrieval.

40 1. Introduction

41 The temperature of the Earth's surface is a fundamental and integral parameter within the
42 larger system of the global climate. Patterns of sea surface temperature (SST) reveal the
43 subsurface ocean variability, while long-term evolution of the global, regional and seasonal
44 averages of SST are potential indicators of climate change (Minnett and Barton 2010). As
45 such, SST is defined as one of the Essential Climate Variables (Bojinski et al. 2014) that
46 critically contributes to the characterization of the Earth's climate by the World
47 Meteorological Organization Global Climate Observing System (GCOS) (WMO 2022).
48 Satellites have been monitoring global surface temperature for several decades, and have
49 established sufficient consistency and accuracy between on-orbit sensors. This includes

50 measurement of the SST, in which case the derived variable is the surface skin temperature
51 (SST_{skin}) (Donlon et al. 2007). However, it is essential that such measurements are fully
52 anchored to the International System of Units (SI) and that there is a direct regular correlation
53 with “true” surface/in-situ based measurements.

54 The most accurate of these surface-based measurements (used for validation) are derived
55 from field-deployed infrared radiometers (or technically ‘radiation thermometers’, although
56 in this article the term ‘radiometer’ will be used following the common usage of the
57 terminology in this field). These are in principle calibrated traceable to SI, generally through
58 a reference standard radiance blackbody (BB) source. Such radiometers are of varying
59 design, operated by different teams in different parts of the globe. It is essential for the
60 integrity of their use, both to provide validation data for satellites on-orbit and to provide the
61 links to future sensors, that any differences in the results obtained between them are
62 understood. This knowledge will allow any potential biases to be removed and not to be
63 transferred to satellite sensors. This knowledge can only be determined through formal
64 comparison of the instrumentation, both in terms of its measurement capabilities in relation to
65 primary “laboratory based” calibration facilities, and its use in the field. The provision of a
66 fully traceable link to SI as part of this process ensures that the data are evidentially robust
67 and can claim their status as a “climate data record”. In Ohring et al. (2005), the target
68 accuracy for satellite-derived SST is given as 0.1 K, and the ship-borne infrared radiometers
69 therefore aim to have similar accuracies, which is better than the measurement requirements
70 for current satellite missions of <0.3 K (Donlon et al. 2012).

71 The calibration and validation community within the Committee on Earth Observation
72 Satellites (CEOS) is well versed in the need and value of such comparisons, and has held
73 highly successful exercises in Miami, Florida in 2001 (Rice et al. 2004, Barton et al. 2004),
74 and at the National Physical Laboratory (NPL), Teddington UK and in Miami in 2009
75 (Theocharous et al. 2010, Theocharous and Fox 2010) and at the NPL in 2016 (Theocharous
76 et al. 2017, Barker-Snook et al. 2017a, Barker-Snook et al. 2017b, Theocharous et al. 2019),
77 all carried out under the auspices of CEOS. However, six years had passed since the last
78 comparison and it was considered timely to repeat/update the process, and so a similar
79 comparison was conducted in 2022. The 2022 comparison included:

80 a. Comparison of the BB reference standards used for calibrating the radiometers
81 (laboratory based).

82 b. Comparison of the radiometer response to a common SI-traceable BB target
83 (laboratory based).

84 c. Evaluation of differences in radiometer response when viewing sea surface targets in
85 particular the effects of external environmental conditions such as sky brightness (field-
86 based).

87 The comparison took place during two weeks in June of 2022. The first week involved
88 the laboratory-based comparisons (a., b.) at NPL. The second week was devoted to the field-
89 based comparison (c.), at the tip of Boscombe Pier in Bournemouth, UK, and this part of the
90 comparison is reported in an accompanying paper (Yamada et al. 2023d).

91 This paper covers the result of the laboratory comparison of both the radiometers of the
92 participants and of the BBs used to calibrate the radiometers. Detail of the comparison results
93 can be found in two reports (Yamada et al. 2023a; 2023b).

94 **2. Overview of the comparison**

95 As in the recent prior comparisons, NPL, the UK National Metrology Institute (NMI),
96 served as the pilot for the 2022 comparison, by coordinating the comparison, preparing the
97 protocol, providing the reference value traceable to the SI, analysing the results, and
98 preparing the reports. The protocol agreed by the participants can be seen in Yamada and Fox
99 (2022). Seven participants including the pilot took part. This is a reduction from the previous
100 2016 comparison where eleven institutes, including the pilot, were present. No institute could
101 participate from the USA and China, primarily due to travel restrictions imposed due to the
102 COVID-19 pandemic.

103 The laboratory comparison was undertaken in the week 13 to 17 June 2022. For the
104 radiometer comparison, participants took turns to measure the reference standard BBs
105 belonging to NPL. These BBs had calibrated platinum resistance thermometers monitoring
106 their temperature which provided the reference value. For the BB comparison, a transfer
107 standard radiometer was used to measure the brightness temperature of the participant BBs.
108 The transfer radiometer was itself calibrated against the NPL reference standard radiometer
109 traceable to the NPL primary temperature standards, and thus served to provide the reference
110 value. Details on the reference standards are provided in the next section.

111 **3 Reference standards**

112 *a. Reference standard BBs*

113 Two variable temperature BBs were utilised in the radiometer comparison. One is an
114 ammonia heatpipe BB (NH3-BB) (Chu and Machin 1999), and the other is a large aperture
115 stirred liquid bath BB (SL-BB) (McEvoy et al. 2024). The comparison reference values are
116 given by the standard platinum resistance thermometers (SPRTs), which are calibrated
117 traceable to the NPL primary temperature standards, measuring the temperature of the BBs.
118 Of the two, the NH3-BB was the same as used in the previous comparison, and a diagram can
119 be found in the paper by Theocharous et al. (2019). In the current comparison, the second BB
120 source (SL-BB) was introduced, so that two measurements could be run side by side dividing
121 the temperature range to be shared by the two BBs for improved efficiency.

122 The specifications for the two NPL variable temperature BBs are shown in Table 1. In
123 recent years the uncertainty for the NH3-BB has been re-evaluated and its day-to-day
124 working uncertainty is slightly increased from what is shown in (Chu and Machin 1999), now
125 being in the range from 0.13 K to 0.10 K below 0 °C and 0.095 K above 20 °C ($k = 2$). The
126 SL-BB has a smaller uncertainty, which is around 0.05 K at 0 °C to 30 °C ($k = 2$), due to its
127 higher emissivity.

128 Both BBs have purge systems utilising a flow of dry nitrogen gas which is used below
129 10 °C. They also have detachable, black-painted apertures which have been applied during
130 the comparison measurements at set-point temperatures below the dew point to prevent
131 ambient air from entering the cavity that can cause condensation of dew and frost. When the
132 aperture is removed at around room temperature, the resulting decrease in cavity emissivity is
133 almost completely balanced by the increase in the cavity reflectance of the ambient radiation,
134 so the same correction and uncertainty due to cavity emissivity have been applied for with
135 and without the aperture.

Table 1 Variable-temperature reference BB specifications

| | NH3-BB | SL-BB |
|------------------------------------|-------------------|---------------------|
| Aperture diameter | ϕ 75 mm max | ϕ 160 mm max |
| Aperture distance from front panel | 75 mm | 35 mm |
| Emissivity | 0.9993@10 μ m | 0.9998 @11 μ m* |
| Temperature range | -40 °C – 50 °C | -10 °C – 40 °C |

136 *: With ϕ 80 mm aperture applied to the cavity opening

137

138 *b. Reference and transfer standard radiometers*

139 The reference standard for the BB comparison was the NPL's reference standard
140 radiometer Absolute Measurements of BB Emitted Radiance (AMBER) (Theocharous et al.
141 1998). In previous comparisons the AMBER was radiometrically calibrated by evaluating the
142 radiance ratio against the gallium (Ga) melting point (29.7646 °C) realised by an NPL
143 reference fixed-point BB (Machin and Chu 1998). When the AMBER views an object the
144 target temperature is derived from the measured radiance ratio. Here, radiance is evaluated as
145 the spectral integration of the Planck's function multiplied by the pre-evaluated relative
146 spectral responsivity function of the instrument. This is analogous to the definition of the
147 ITS-90 above the silver point (Preston-Thomas 1990), although applied at a much lower
148 temperature. The calibration had previously been verified through comparison with
149 Physikalisch-Technische Bundesanstalt (PTB), Germany (Gutschwager et al. 2013).
150 However, the scheme requires the knowledge of the zero-radiance signal that is derived
151 through measurement of a zero-radiance source such as a cryogenic blackbody, which is hard
152 to implement in practice. For the current comparison exercise, a new calibration scheme was
153 applied employing a second reference temperature at around -30 °C through measurement of
154 the NH₃-BB, and extrapolating down to determine the zero-radiance signal, thus rendering
155 the problematic realisation of the zero-radiance source unnecessary. A detailed description of
156 this two-point interpolation scale realization is described in a separate article (Yamada et al.
157 2023e).

158 A transfer standard radiometer was introduced for the first time in this comparison, which
159 was the NPL TRT-IV.82 manufactured by Heitronics Infrarot Messtechnik GmbH
160 (hereinafter referred to as 'Heitronics'). This transfer standard was introduced following the
161 positive contribution to the previous comparison by a radiometer of a similar model
162 belonging to PTB (Theocharous et al. 2017). The Heitronics transfer standard radiometer was
163 calibrated by comparison against the AMBER reference standard utilising as the comparator
164 sources the same NPL variable temperature NH₃-BB and SL-BB described above. Then the
165 Heitronics transfer standard was used to measure the temperature of the participant BBs.

166 The AMBER has a relatively small but not insignificant size-of-source effect (SSE).
 167 Therefore, a correction was made to account for the difference in the size of the two sources
 168 used for scale realisation (30 mm diameter for the Ga-point BB and 75 mm diameter for the
 169 NH3-BB) and the AMBER SSE. For the Heitronics, a correction was made for the effect of
 170 the difference in the source size of the NH3-BB used to calibrate the Heitronics by
 171 comparison with the AMBER, and the participants' BB sizes. For this, a SSE correction
 172 scheme was applied that enables correction up to large source sizes at all measurement
 173 temperatures, based on a method described in Bloembergen (1999). The stability of the
 174 Heitronics was monitored by measurement of the Ga-point BB a few times a day before and
 175 during the comparison period. An abrupt shift of approximately 70 mK was detected after the
 176 calibration and just before the comparison, and a correction was applied to the measurements
 177 made of the participants' BBs to account for this. The uncertainty in this correction was also
 178 included in the uncertainty of the reference temperature.

179 The specifications of the AMBER and Heitronics relevant to the comparison
 180 measurements are given in Table 2.

181 Table 2 Reference and transfer standard radiometer specifications

182

| | AMBER (reference standard radiometer) | Heitronics TRT-IV.82 (transfer standard radiometer) |
|--------------------------------|---|--|
| Wavelength | 10.1 μm (9 μm – 11 μm) | 8 μm - 14 μm |
| Target size | ϕ 5 mm | ϕ 8.7 mm |
| Measurement distance | 70 mm | 503 mm |
| Effective window/lens diameter | ϕ 13 mm | ϕ 57 mm |
| Scale realization | Through relative spectral response measurement, and BB measurement at the Ga melting point and at a second reference temperature at -30 °C. | By comparison with AMBER |

183

184 **4. Participants' instruments**

185 *a. BBs*

186 There are, in general, two types of BBs used for calibration of radiometers for SST_{skin}
187 retrieval. One is a BB cavity immersed in a stirred liquid bath, and the other is a BB cavity
188 formed in a metal block. The BBs that participated in this comparison all belong to one of
189 these two types. None of the BBs had a purge system to prevent formation of dew and frost.
190 Therefore, their operation was limited to above the dew point of the laboratory, which was
191 just below 10 °C during the comparison.

192 1) SPECIALISED BB WITH CAVITY IN STIRRED LIQUID BATH

193 BBs of the stirred liquid bath type that participated in the comparison are the CASOTS
194 (Donlon et al. 1999) and CASOTS-II (Donlon et al. 2014) BBs. Both are similar in
195 configuration and operation, the difference being in the improved thermal insulation leading
196 to better temperature uniformity for the latter. The BB consists of cylindroconical cavity of
197 copper with internal black coating of NEXTEL Suede Coating (NEXTEL Velvet Coating for
198 CASOTS), leading to a high estimated emissivity of 0.99981 with a 50 mm diameter aperture
199 plate (CASOTS-II). The bath has no temperature control and the adjustment is made by
200 adding or removing hot water, cold water or ice. The temperature of the bath is monitored by
201 a thermistor or a platinum resistance thermometer.

202 The Science and Technology Facilities Council (STFC) Rutherford Appleton Laboratory
203 (RAL) brought with them their CASOTS, while University of Southampton (UoS) and
204 CSIRO / Australian Bureau of Meteorology (CSIRO) took part in the comparison with their
205 CASOTS-II.

206 2) COMMERCIAL BB WITH CAVITY IN METAL BLOCK

207 Two participants participated with the same commercial BB system (Manufacturer:
208 AMETEK-LAND, Model: Landcal P80P). This system comprises a cylindroconical BB
209 cavity with black, high temperature refractory coating in an aluminium block to achieve an
210 emissivity higher than 0.995. The temperature of the block, heated and cooled by Peltier
211 elements, can be monitored by a platinum resistance thermometer.

212 University of Valencia (UoV) and Karlsruhe Institute of Technology (KIT) participated in
213 the BB comparison with this type.

214 *b. Radiometers*

215 The radiometers that participated in this comparison can be categorised in to two types:
216 dedicated systems for SST_{skin} retrieval equipped with internal BB references, and systems
217 based on a commercially available instrument for general use without internal BB references.
218 Other types of radiometer that were present in the previous comparison, such as Fourier-
219 Transform Infrared Spectroradiometer type, were not among those that participated this time.

220 1) DEDICATED SYSTEMS FOR SST_{SKIN} RETRIEVAL WITH INTERNAL BBS

221 The SISTeR radiometer (Barton et al. 2004, Theocharous et al. 2019) of RAL, and ISAR
222 radiometer (Donlon et al. 2008) manufactured by UoS belong to the category of radiometer
223 with an internal BB. Both have two reference BB cavities, one at ambient temperature, and
224 the other, with a constant heater power supplied, at a slightly higher temperature
225 (approximately 12 K higher for ISAR, and 17 K higher for SISTeR). Both have a 45 °
226 scanning mirror that deflects the field of view of the radiometer to successively measure the
227 radiation from the sea, the sky and the two BBs. ISAR's detection is made by use of a
228 radiometer (Manufacturer: Heitronics, Model: KT15.85) with detecting wavelength range
229 from 9.6 µm to 11.5 µm. SISTeR utilised a pyroelectric detector in combination with a
230 bandpass filter centred at 10.85 µm with full width at half maximum of 0.88 µm.

231 RAL participated with SISTeR, while UoS, CSIRO and the Danish Meteorological
232 Institute (DMI) participated with various models of ISAR. For all ISAR models the optics
233 and the detectors are of the same design.

234 2) COMMERCIAL INSTRUMENTS WITHOUT INTERNAL BB REFERENCE

235 Two institutes participated with radiometers of the category without internal BBS. KIT
236 brought a set of two radiometers (KIT-1, KIT-2, Manufacturer: Heitronics, Model:
237 KT15.85 IIP) with wavelength range from 9.6 µm to 11.5 µm. One was intended for sea
238 surface radiance measurement while the other was intended for sky radiance measurement.
239 Similarly, UoV took part with a set of two radiometers (manufacturer: CIMEL Electronique,
240 model: CE312-2), each with six selectable spectral bands (B1: 8.0 µm to 13.3 µm, B2:
241 10.9 µm to 11.7 µm, B3: 10.2 µm to 11.0 µm, B4: 9.0 µm to 9.3 µm, B5: 8.5 µm to 8.9 µm,
242 and B6: 8.3 µm to 8.6 µm) utilising thermopile detectors. In this comparison each of these
243 bands was treated as an independent participating instrument. A summary of the participants'
244 instrumentation is given in Table 3.

245 Table 3 Participants' BBs and radiometers. Acronyms are used in graphs. UoV-1 and 2
 246 radiometers each have 6 bands, which have acronym extensions from B1 to B6 and each band
 247 is treated as an independent instrument in the comparison.

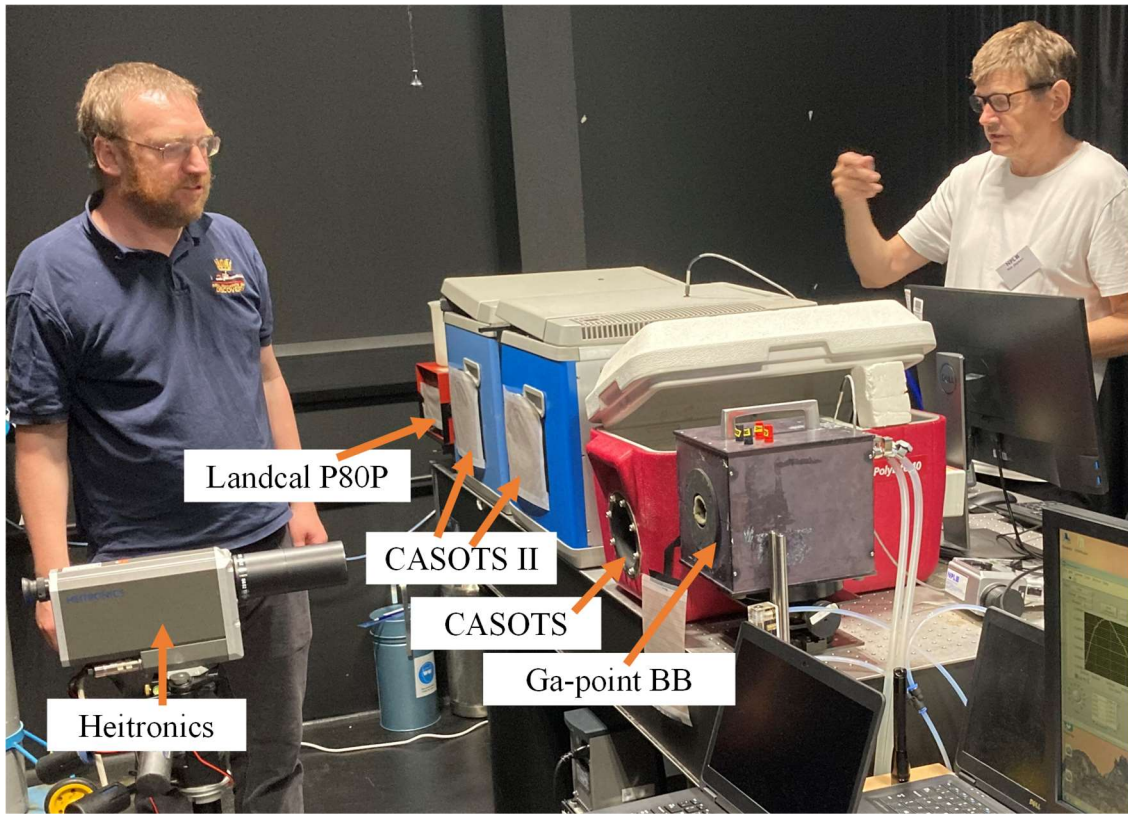
248

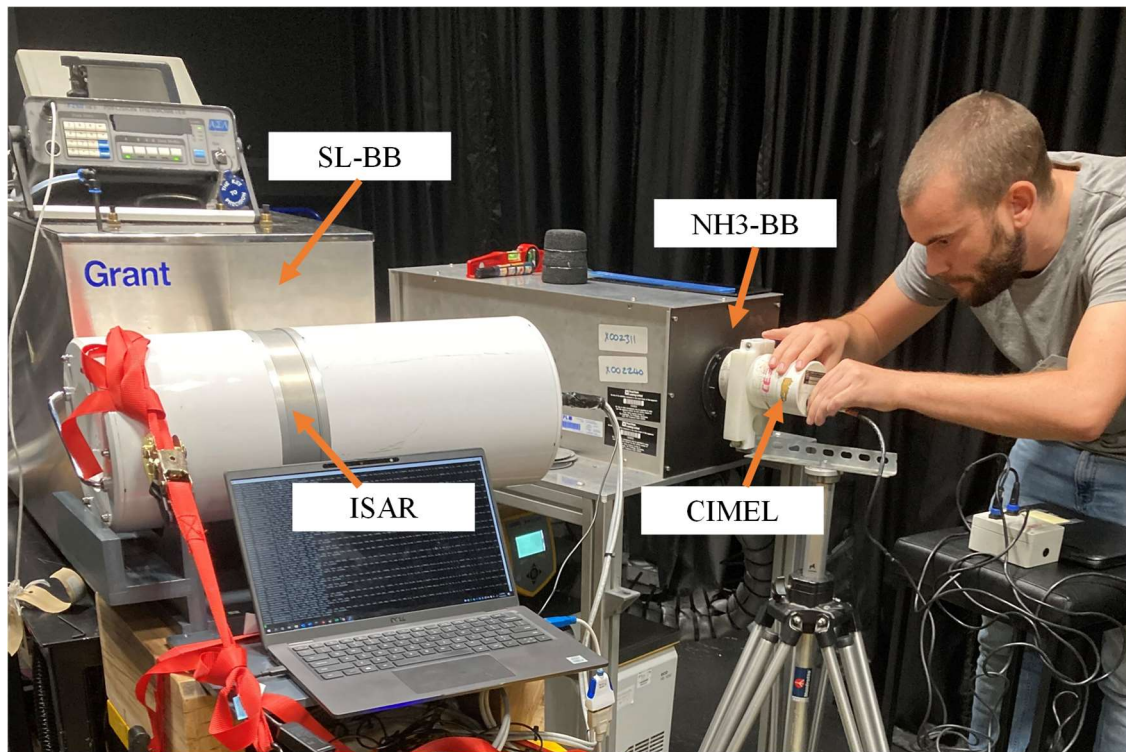
| Institute | BB | | Radiometer | |
|--|--------------|---------|--------------------------------|-------------|
| | Model | Acronym | Model | Acronym |
| University of Valencia | Landcal P80P | UoV | CIMEL Electronique CE312-2 | |
| | | | Unit 1 | UoV-1 B1-B6 |
| | | | Unit 2 | UoV-2 B1-B6 |
| Karlsruhe Institute of Technology | Landcal P80P | KIT | Heitronics KT15.85 IIP | |
| | | | SN #9353; 'surface' radiometer | KIT-1 |
| | | | SN #13794; 'sky' radiometer | KIT-2 |
| CSIRO / Australian Bureau of Meteorology | CASOTS-II | CSIRO | ISAR5-E serial number 16 | CSIRO |
| University of Southampton | CASOTS-II | UoS | ISAR5-C serial number 3 | UoS |
| STFC Rutherford Appleton Laboratory | CASOTS | RAL | SISTeR | RAL |
| Danish Meteorological Institute | — | — | ISAR-5D | DMI |

249

250 A view of the laboratory where the BB comparison was carried out is shown in Fig. 1 a).
 251 On the left, the NPL transfer radiometer (Heitronics) is shown viewing the reference standard
 252 compact Ga-point BB placed on the optical bench. On the left of the Ga-point BB a red
 253 CASOTS BB is seen, together with two blue CASOTS-II BBs to its left. At the far end of the

254 row of BBs a Landcal P80P BB is seen. A second Landcal P80P was present but is not shown
255 in the photograph. A view of the laboratory during the comparison of radiometers is shown in
256 Fig. 1 b). On the left, the CSIRO ISAR radiometer is measuring the SL-BB. On the right, the
257 UoV CIMEL radiometer is being set up to measure the NH3-BB.





259 b)

260 Figure 1 View of laboratory during comparison measurements. a) BB comparison from far
 261 left: Landcal P80P, CASOTS-II, CASOTS-II, CASOTS, Ga-point BB. Facing the BBs is the
 262 Heitronics transfer radiometer. b) Radiometer comparison measurements from left: ISAR
 263 measuring the SL-BB, Right: CIMEL being prepared for NH3-BB measurement.

264

265 5. Measurement temperatures and measurand

266 In both the BB and the radiometer comparisons, the principle measurand was the brightness
 267 temperature of the BB sources at 10 μm . Therefore, where the temperature values are derived
 268 from contact thermometers monitoring the BB (as in the case of participant reported values in
 269 BB comparison, and pilot reference value in the radiometer comparison) corrections in the
 270 brightness temperature are required for source emissivity and ambient reflection. Where
 271 temperatures are measured by a 10 μm -range radiometer (as in the participant reported value
 272 in the radiometer comparison, and the pilot reference value in the BB comparison) corrections
 273 are required for the SSE of the radiometer (when possible) but nothing else. Temperature here
 274 refers to that on the International Temperature Scale of 1990 (ITS-90) (BIPM 1989).

275 a. BB comparison

276 For the BB comparison the participants' BBs were compared at the nominal temperatures
 277 covering the range from 10 °C to 50 °C as shown in Table 4 using the Heitronics transfer
 278 standard radiometer. All BBs participated at all temperature points up to 35 °C, above which
 279 only two participants (KIT, UoV) participated. Measurements at 55 °C and 60 °C were also
 280 made by KIT, but these are not considered a part of the comparison since AMBER and
 281 Heitronics were not calibrated prior to the comparison up to these temperatures and
 282 measurement uncertainties with these instruments at these temperatures were not available.

283 *b. Radiometer comparison*

284 For the radiometer comparison the NPL BBs were set at the nominal temperatures covering
 285 the range from –30 °C to 50 °C as shown in Table 4. The temperature range of main interest
 286 for SST_{skin} retrieval is 10 °C to 30 °C, so the SL-BB, having better temperature stability and
 287 higher emissivity as well as larger aperture for ease in alignment, was assigned to cover this
 288 range. The NH3-BB, being able to rapidly change set-point temperature and covering a wider
 289 range, was assigned to cover the higher and lower ends. At 0 °C and 30 °C, both BBs were
 290 measured so that a check could be made of the agreement of the radiometer measurements
 291 made with the two BBs. All participants participated in all temperature points except at 50 °C,
 292 where only UoV, KIT and RAL participated. However, CSIRO later withdrew from submitting
 293 their results for three of the points (–15 °C, 35 °C and 40 °C) after noticing an issue with the
 294 alignment of their radiometer against the NH3-BB.

295 Table 4 Measurement temperature points. Italic fonts represent temperature points where
 296 limited number of participants made measurements.

| Comparison type | Nominal temperature / °C |
|-----------------------|--|
| BB comparison | 10, 15, 20, 25, 30, 35, <i>40, 45, 50</i> , (<i>55, 60</i>)* |
| | *: Outside the scope of comparison |
| Radiometer comparison | |
| NH3-BB source | –30, –15, 0, 30, 35, 40, <i>50</i> |
| SL-BB source | 0, 10, 20, 30 |

297

298 **6. Measurement and reporting**

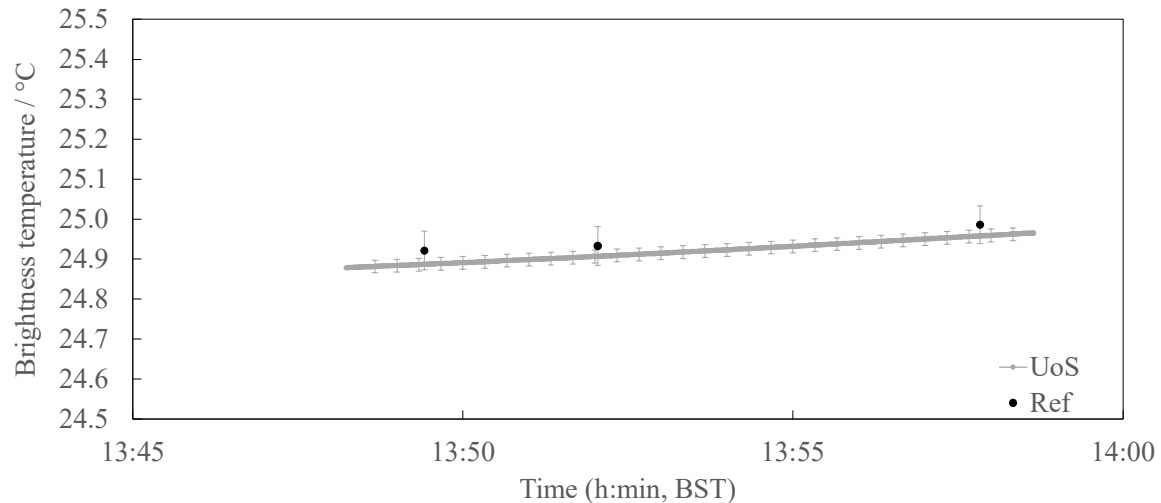
299 *a. BB comparison*

300 The participants set the BBs to the set-point temperature and, when the temperature was
301 sufficiently stable, the pilot took measurements of the BB brightness temperature with the
302 transfer standard Heitronics radiometer. At least three repeated measurements were made
303 with the Heitronics, including a re-alignment. The participants themselves took
304 measurements of the BB temperature through contact thermometers. This was continuously
305 logged for CASOTS and CASOTS-II BBs, and time stamped data was reported. For the P80P
306 BBs it was checked that the BB temperature stayed constant during the pilot's measurement.

307 Participants reported values of BB temperature after correcting for the BB emissivity and
308 for the ambient reflection. The values measured with the transfer standard Heitronics by the
309 pilot were corrected both for the difference from the reference AMBER scale, and for the
310 Heitronics' SSE to account for the difference in the size of the source used to calibrate the
311 transfer radiometer and the size of each of the participants' BBs. The SSE was measured with
312 a flat plate radiator as a source in front of which apertures with varying diameters were
313 placed, with sufficient space and tilt between them to prevent multiple reflections. The
314 method for the SSE correction follows that presented by Bloembergen (1999), which allows
315 correction to be applied to temperatures at which SSE is not directly evaluated. Heitronics
316 temperature values after the corrections became the reference brightness temperatures of the
317 BBs. The mean of the differences between the three reference brightness temperature values
318 and the participant temperature values made at the same time was evaluated, and the
319 reproducibility was assessed and included in the comparison uncertainty. When the
320 participant reported a single value instead of temporal data the difference of this value from
321 the simple mean of the reference measurements was used. Participants reported uncertainties
322 of the measurement accompanying each measured value. The uncertainties included such
323 sources as BB emissivity uncertainty, thermometer calibration uncertainty, cavity
324 temperature non-uniformity, BB temperature stability, and reflected ambient radiation, as
325 well as Type A uncertainties. Details of the uncertainty estimations are found in Yamada et
326 al. (2023a).

327 An example of measurement data from a participant BB with the transfer radiometer is
328 shown in Fig. 2. Here, the UoS CASOTS-II BB is measured intermittently by the Heitronics
329 while the water bath temperature is continuously monitored by a thermistor. The logging of
330 the data was done on two separate computer systems whose clocks were synchronized prior

331 to data acquisition. CASOTS-II BB does not have temperature control capability, so the
332 temperature is seen to gradually heat up due to the heat generated by the bath stirrer pump.
333 The transfer standard Heitronics radiometer measurement is seen to follow this trend. Since
334 the data acquisition synchronization (better than 30 s) is well within the time for significant
335 temperature drift (at a rate of less than 0.01 °C/min), the change in BB temperature has
336 insignificant effect on the measurement.



337
338 Figure 2 An example of measurement data of participant’s BB brightness temperature. UoS
339 CASOTS-II BB at a nominal temperature of 25 °C measured by a thermistor monitoring the
340 water bath temperature (‘UoS’) and by the transfer standard Heitronics radiometer (‘Ref’).
341 Error bars denote standard uncertainties.

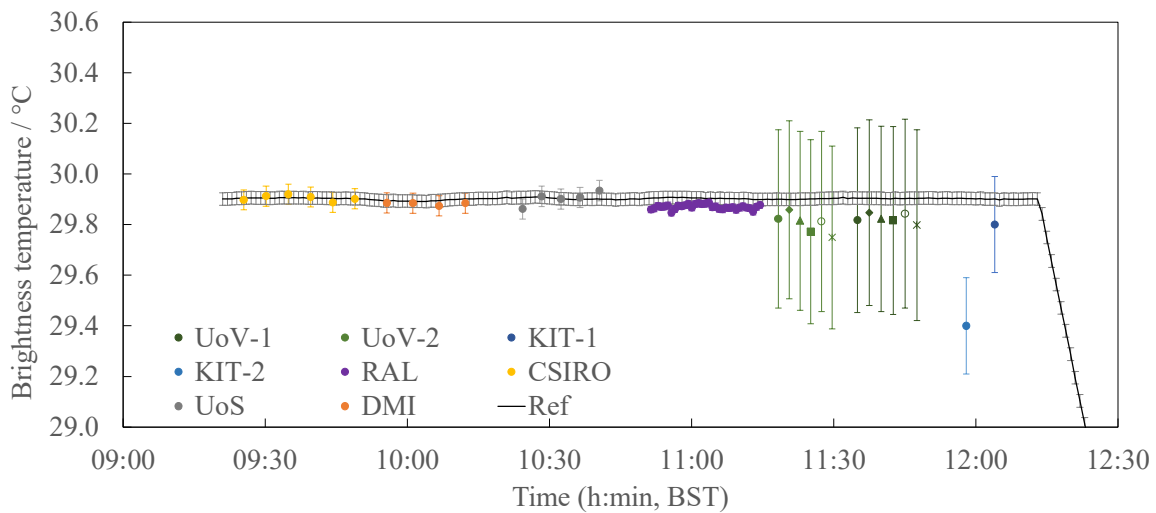
342

343 *b. Radiometer comparison*

344 The participants took turns to align and measure the NPL BBs, with their radiometers,
345 when the BB temperature was stable at the set-point. The pilot measured the BB temperature
346 continuously with SPRTs whose calibration was traceable to the NPL primary temperature
347 standards, with corrections to the temperature applied for the cavity emissivity and ambient
348 reflection to derive the reference brightness temperature value. The participants reported the
349 time-stamped measured brightness temperature values and the associated uncertainties. The
350 uncertainties included such sources as the primary calibration uncertainty of the radiometer,
351 linearity, drift since calibration, and ambient temperature effect, as well as Type A
352 uncertainties. Details of the uncertainty estimations reported by each participant are found in

353 Yamada et al. (2023b). The measurements reported by the participants were compared with
 354 the reference value at the same point in time. The mean of the differences of the temperature
 355 values corresponding to the same timing was evaluated and the uncertainty of the mean was
 356 included in the comparison uncertainty.

357 An example of the measurement data of the reference SL-BB with participant radiometers
 358 is plotted in Fig. 3.



359
 360 Figure 3 An example of measurement data of the reference BB brightness temperature.
 361 NPL’s SL-BB at a nominal temperature of 30 °C is measured by reference SPRT monitoring
 362 the water bath temperature (‘Ref’) and by participants’ radiometers. Error bars denote
 363 standard uncertainties. For both UoV-1 and UoV-2 radiometers, each plot corresponds to a
 364 spectral band, from B1 to B6 in this order from left to right.

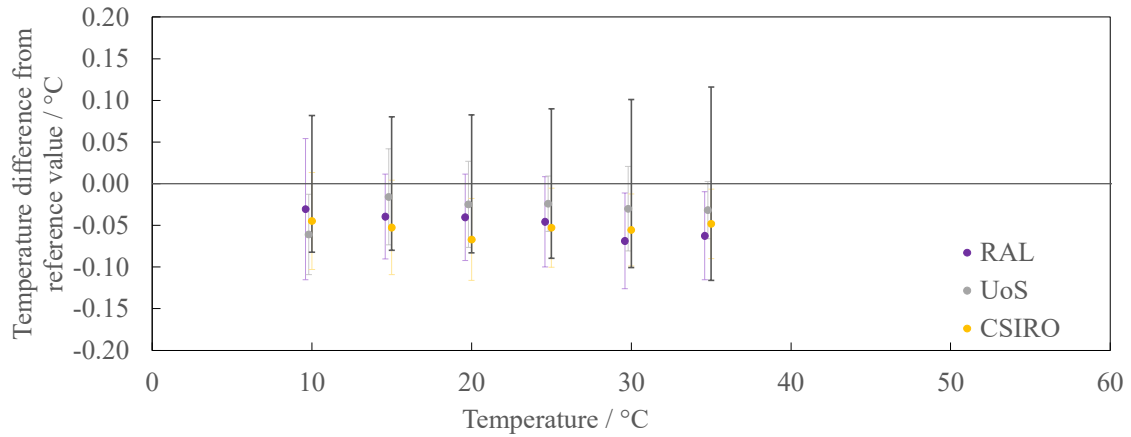
365

366 7. Comparison results

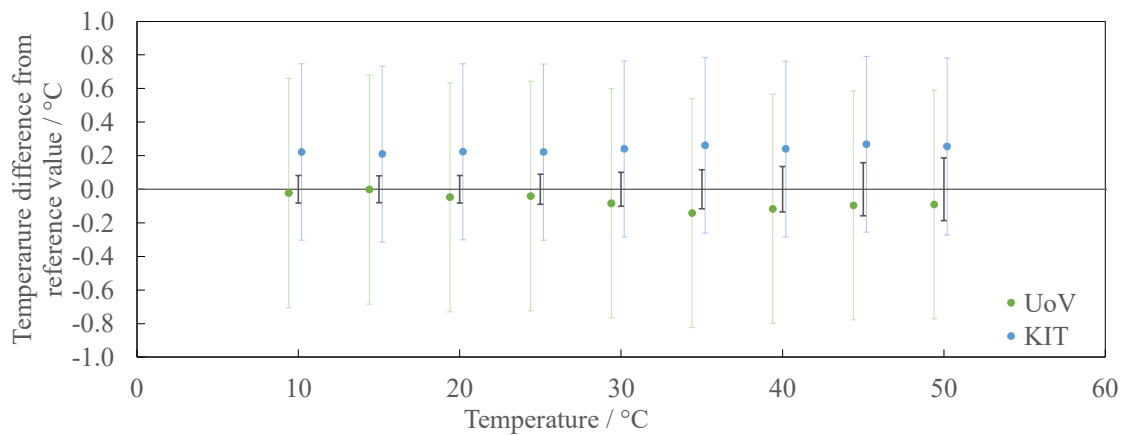
367 a. BB comparison result

368 Agreement with the reference value is evaluated by plotting the data with error bars added
 369 to both the participant reported values and the reference values, as shown in Figs. 4 a) and b).
 370 The error bars are the expanded uncertainties ($k = 2$). Plots are shifted slightly to make them
 371 distinguishable.

372 Since the CASOTS and CASOTS-II BBs have significantly smaller reported uncertainties
 373 than those for the other participant BBs, Fig. 4 a) show results for these BBs, while Fig. 4 b)
 374 shows those for the others. Note the difference in the vertical scales.



375 a)



376 b)

377 Figure 4 BB comparison result. Error bars denote expanded uncertainty ($k = 2$). The
 378 expanded uncertainties of the reference values are the black bars. a) Specialised BBs
 379 (CASOTS and CASOTS-II). b) Commercial BBs (Landcal P80P)

380

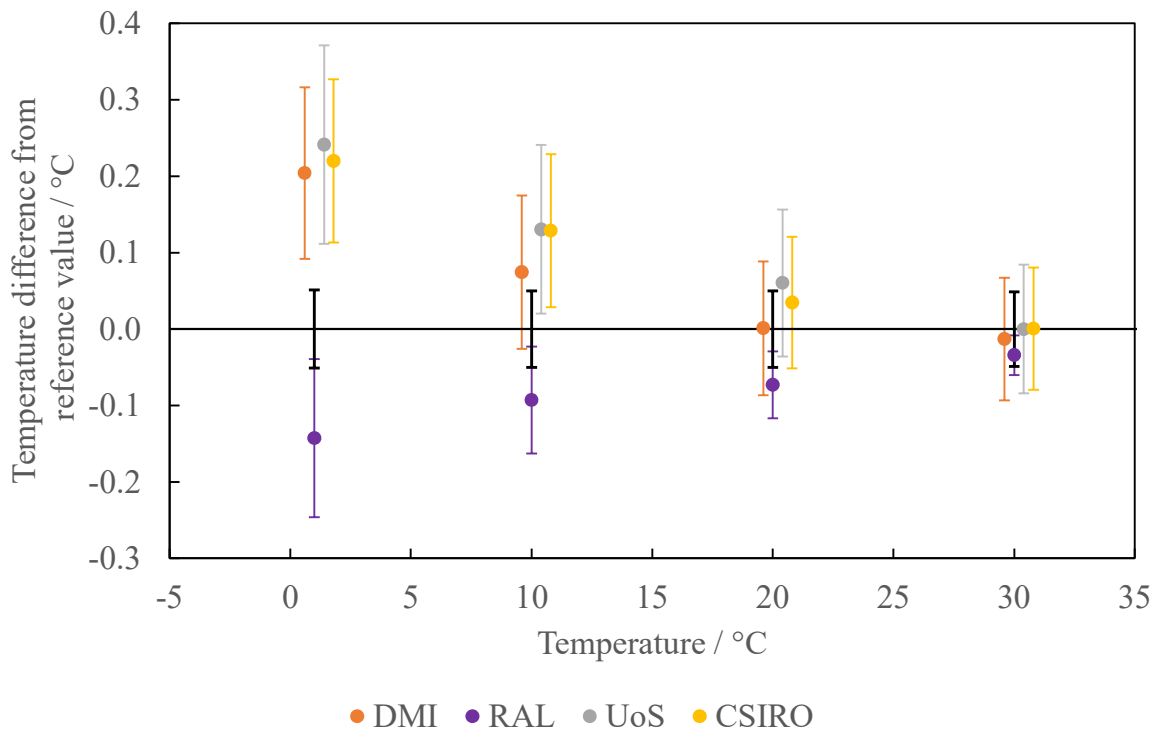
381 b. Radiometer comparison result

382 Agreement with the reference value is evaluated by plotting the data with error bars added
 383 to both the participant reported values and the reference values, as shown in Fig. 5 and Fig. 6.
 384 Plots are shifted slightly to make them distinguishable. The error bars are the expanded
 385 uncertainties ($k = 2$). At each temperature point, each participant reported either a set of time
 386 stamped measurements or a single averaged value. For the former, evaluation of the standard
 387 error of the mean of the temperature difference from the reference was evaluated for each set

388 of measurements, and this was combined with the participant claimed combined
389 measurement uncertainty.

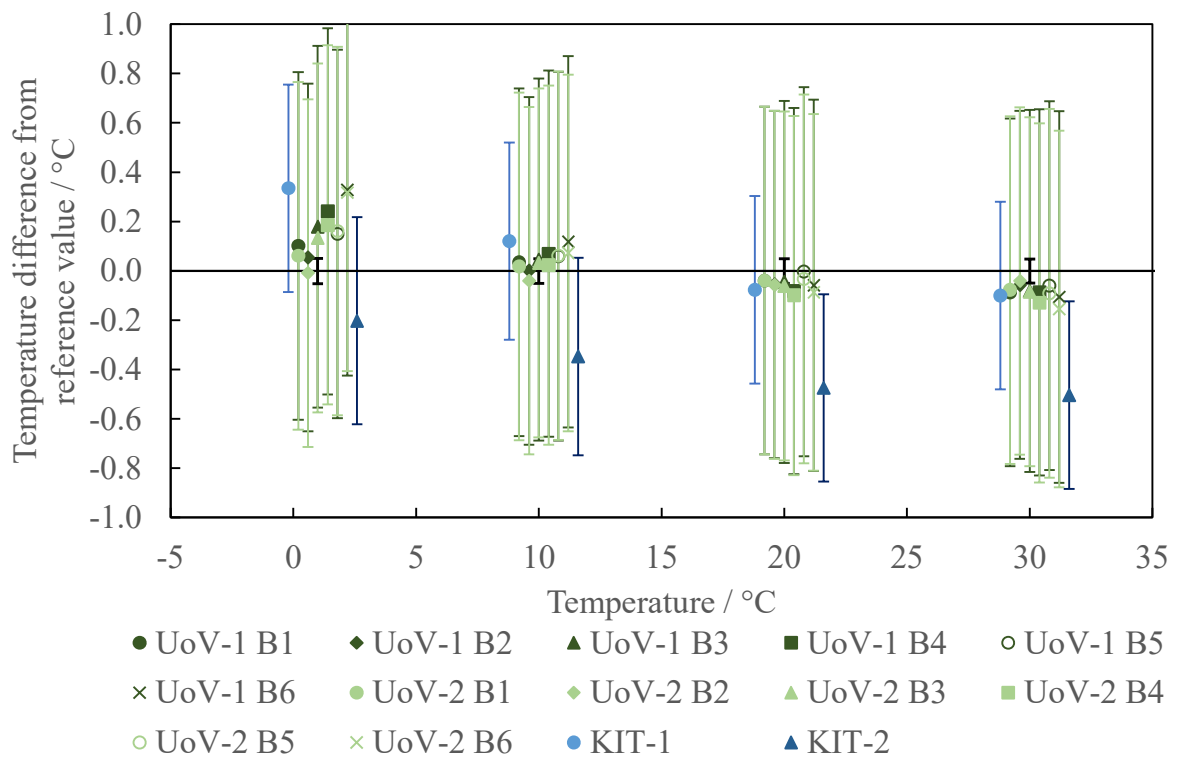
390 Since the ISAR and SISTeR radiometers have an internal reference BB to improve the
391 accuracy of measurement, the quoted uncertainties are significantly smaller than for the other
392 two types of radiometer. Therefore, Fig. 5 a) and Figs. 6 a) and b) show results for the ISAR
393 and SISTeR instruments, while Fig. 5 b) and Fig. 6 c) show those for the others. Note the
394 difference in the vertical scales.

395 a)



396

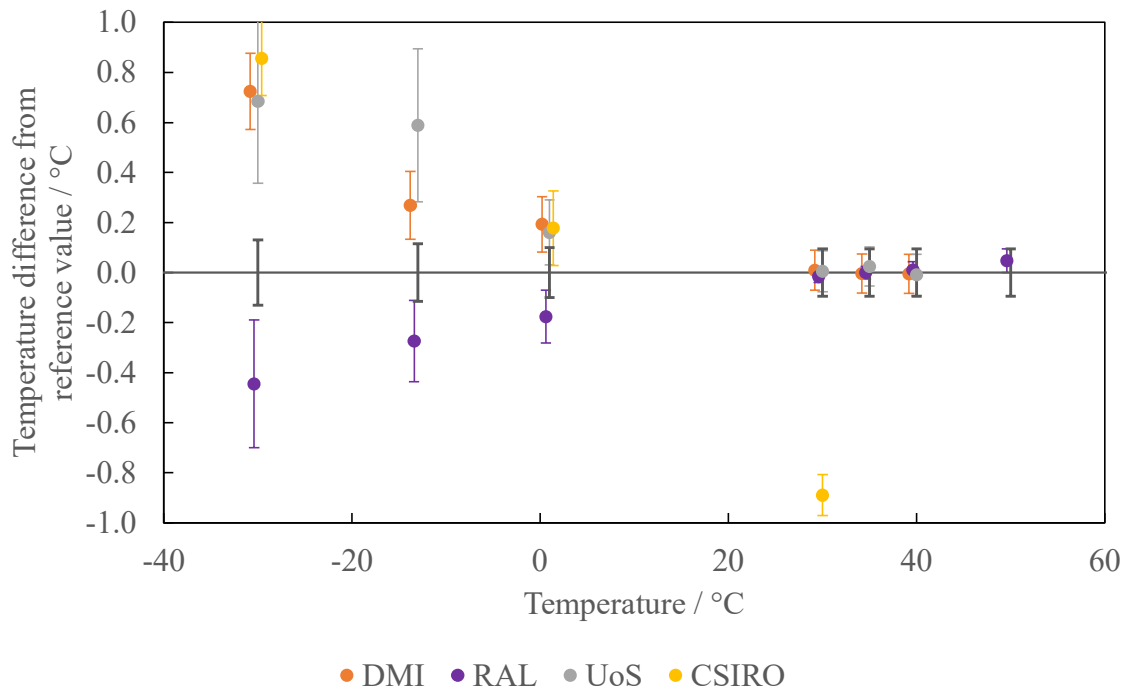
397 b)



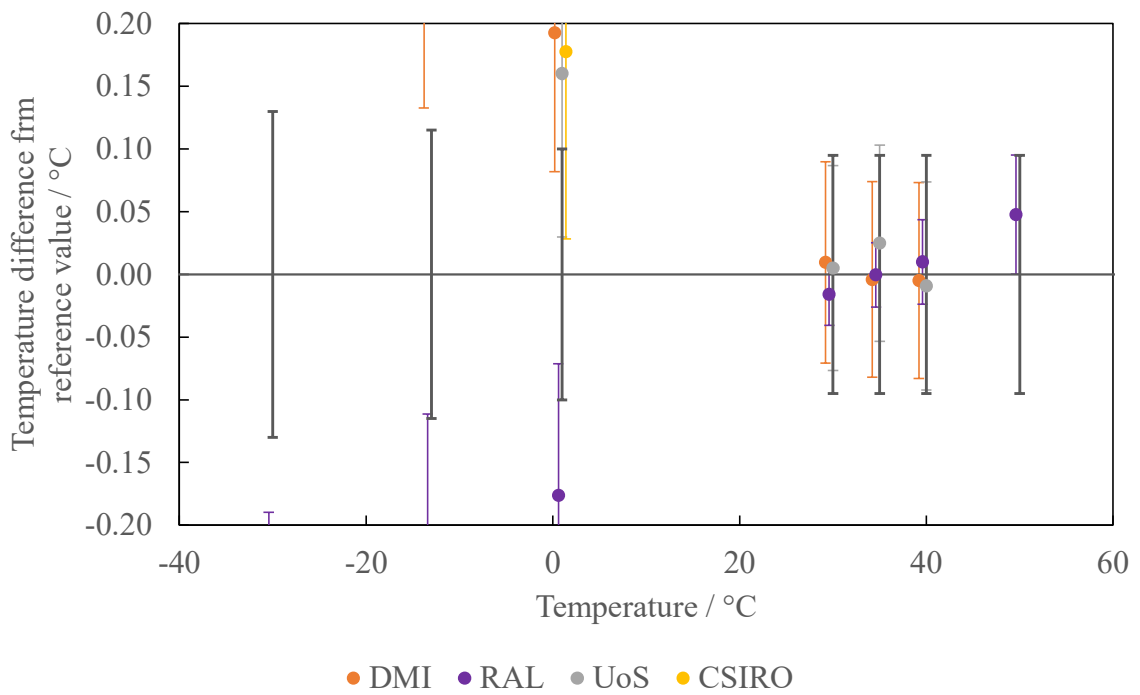
398

399 Figure 5 Radiometer comparison result with SL-BB. Error bars are the expanded
400 uncertainties ($k = 2$) for the participant measured values and for the reference value (latter
401 shown as black bars). Plots are shifted slightly to make them distinguishable. a) CSIRO, UoS,
402 RAL and DMI radiometers. b) UoV and KIT radiometers.

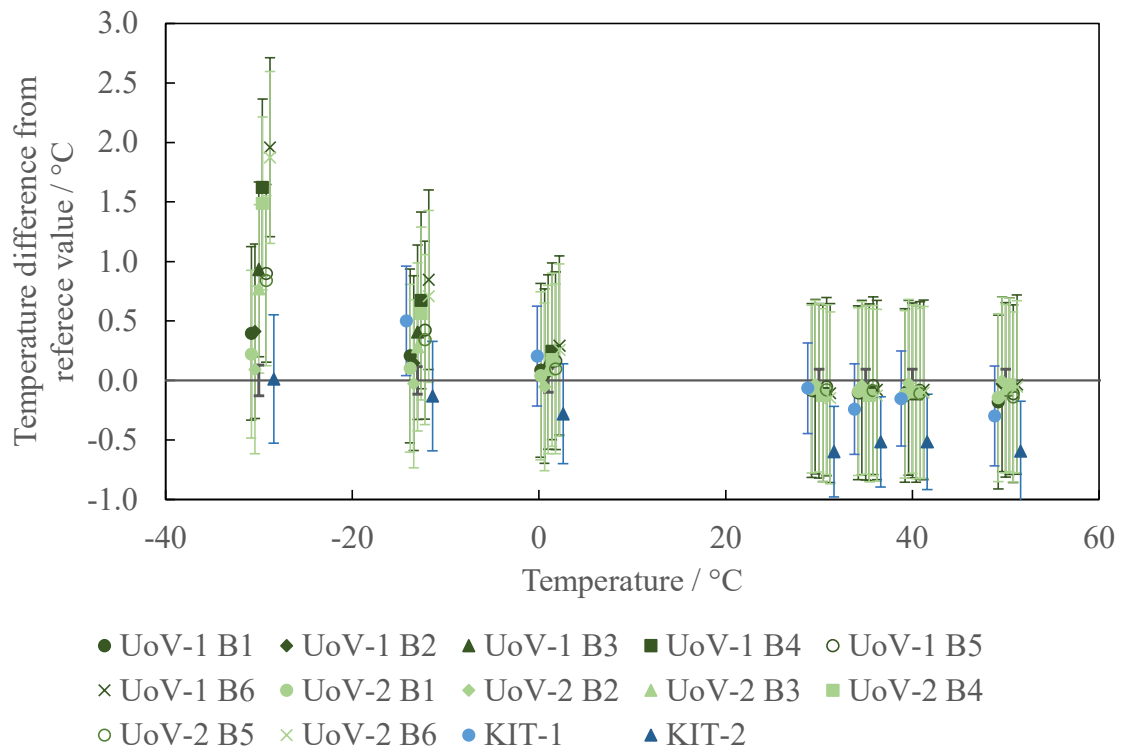
403



404 a)



405 b)



406 c)

407 Figure 6 Radiometer comparison result with NH3-BB. Error bars are the expanded
 408 uncertainties ($k = 2$) for the participant measured values and for the reference value (latter
 409 shown as black bars). Plots are shifted slightly to make them distinguishable. a) CSIRO, UoS,
 410 RAL and DMI radiometers. b) CSIRO, UoS, RAL and DMI radiometers (magnified vertical
 411 scale). c) UoV and KIT radiometers.

412

413 8. Discussions

414 a. BB comparison

415 Figure 2 shows an example of a measurement of the CASOTS-II BB, which is the type
 416 with the BB cavity immersed in a stirred bath. The figure shows that, although the BB
 417 temperature is slowly fluctuating, the Heitronics' reading follows the temporal fluctuation of
 418 the monitored BB temperature. The figure also verifies that the stability of the participant
 419 CASOTS-II BB is sufficient as long as the timings of the temperature readings are matched
 420 with the timings of the radiometric measurements, as is done in the current comparison. The
 421 other BB type, with the cavity in a temperature-controlled metal block (the Landcal P80P), is
 422 believed to have stable enough temperature control to assume its temperature to be constant,

423 although this was not verified from the data since no temporal data were provided by the
424 participants. In the case of the UoV BB, the stability was studied, before the comparison,
425 using external PRT readings at fixed BB temperatures (10 °C, 20 °C, 40 °C and 50 °C) during
426 90 min, obtaining a maximum standard deviation value of 0.03 K.

427 The standard measurement uncertainty with the Heitronics, including the scale realisation
428 on the AMBER, was approximately 45 mK at 20 °C, which is comparable to or slightly
429 smaller than the 53 mK reported for AMBER in the previous comparison (Theocharous
430 2017). This is due mainly to the employment of the novel two-point interpolation scale
431 realisation on the AMBER, and the improved short-term stability and reproducibility
432 achieved by using the Heitronics as the transfer standard for the comparison measurements.
433 The short-term repeatability of the Heitronics was good and including this uncertainty term
434 did not increase the calibration uncertainty.

435 Figure 4 a) shows that the deviations of the participant reported temperatures for the
436 CASOTS and CASOTS-II BBs (belonging to RAL, UoS and CSIRO) from the reference
437 (brightness temperature) values are relatively small and are all less than 50 mK. The Landcal
438 P80P BBs (of UoV and KIT) show larger deviations exceeding 0.1 K in some cases (Fig. 4
439 b)). No apparent dependence of the deviations on BB temperature is observed. The Landcal
440 P80P BBs have an emissivity of 0.995 (cf. section 3. a), and may be affected by reflection of
441 objects that are at different temperatures from the ambient.

442 In the figures, the error bars, corresponding to the expanded participant and reference
443 value uncertainties ($k = 2$), overlap with each other, confirming the agreement with the
444 reference value within the uncertainties for all BBs at all temperatures. The uncertainty of the
445 reference is larger than the claimed uncertainties for the CASOTS and CASOTS-II BBs, but
446 the former is sufficiently small to claim the comparison supports the reliability of the
447 compared artefacts.

448 The temperature range of comparison for the CASOTS and CASOTS-II BBs was from 10
449 °C to 35 °C, and good agreement with the reference value was confirmed in this range. This
450 range is largely sufficient for the intended application, namely SST_{skin} retrieval. If similar
451 accuracy is to be required for ice or land surface temperature retrieval, the BB operation
452 temperature range needs to be expanded. It should be noted that formation of dew and frost
453 will not be an issue if the ambient temperature can also be lowered together with the set point

454 so that it corresponds better to the actual condition in the field, for by doing so the dew point
455 will also be lowered.

456 *b. Radiometer comparison*

457 Figure 3 shows that the stability of the reference SL-BB was sufficient to evaluate the
458 agreement of the participants' temperature scales with the SI. For both this BB and the NH3-
459 BB, the evaluated standard errors of the mean for each set of measurements were all small
460 enough that including these only increased the combined uncertainty by less than 5 %.
461 Exceptions were some cases at $-15\text{ }^{\circ}\text{C}$ and $-30\text{ }^{\circ}\text{C}$, but, for these extreme cases, it could be
462 confirmed from the scatter of the data that the poor repeatability was caused by the
463 radiometer and not the reference BB. For the temperature range from $0\text{ }^{\circ}\text{C}$ to $30\text{ }^{\circ}\text{C}$, which is
464 of most interest from the SST_{skin} retrieval objective, the SL-BB was used, and the
465 introduction of this additional reference source for this comparison has made a positive
466 impact through its exceptional stability.

467 In Fig. 5 and Fig. 6, the agreement of the participants' values with the reference value is
468 evaluated. The expanded uncertainties ($k = 2$) are expressed by error bars for both the
469 participant measurements and for the reference. Overlap of the error bars for the
470 measurement and the reference value, indicating the agreement of the two, is confirmed for
471 all participants in the range $10\text{ }^{\circ}\text{C}$ to $30\text{ }^{\circ}\text{C}$. The main source of the uncertainty for the UoV
472 and KIT radiometers corresponds to the primary calibration uncertainty (from the Landcal
473 P80P BB used), which was estimated as 0.34 K for UoV and 0.15 K for KIT ($k = 1$, cf. Fig. 4
474 b)), and was mainly due to the BB cavity temperature non-uniformity effect. However, the
475 good agreement observed in the comparison result indicates this is likely an overestimation.
476 This is further confirmed in the BB comparison (Fig. 4). Investigation is envisaged to
477 determine a more realistic reduced calibration uncertainty.

478 Separate graphs of the differences of the participant values from the reference value are
479 given for the two sources, the SL-BB (Fig. 5) and the NH3-BB (Fig. 6). At $0\text{ }^{\circ}\text{C}$ and $30\text{ }^{\circ}\text{C}$
480 both sources are measured by the radiometers, and it can be verified that the two sources are
481 practically equivalent, i.e., the differences (participant value – reference value) agree. The
482 single outlier at these two temperatures is the measurement by CSIRO of the NH3-BB at
483 $30\text{ }^{\circ}\text{C}$, which shows an almost $1\text{ }^{\circ}\text{C}$ lower value than with the SL-BB. This is most likely
484 caused by an issue with the alignment of the radiometer against the NH3-BB aperture, the

485 wide field of view of the radiometer not being fully contained within the aperture that is
486 located deep inside from the BB front face.

487 In Fig. 5 and Fig. 6, results for the ISAR and SISTeR radiometers are plotted separately
488 from the other instruments with larger uncertainties. It is clear from the graphs that all three
489 ISARs agree very well with each other while the SISTeR shows a different trend. A
490 systematic error in the ISAR instrument may be present. An investigation into the cause is
491 recommended for improved reliability.

492 In Fig. 5 and Fig. 6, it can also be seen that the scatter of the data increases as the
493 temperature becomes lower, and also larger differences from the reference are observed. This
494 is natural since the detected radiance signal of the radiometers becomes lower and the signal-
495 to-noise ratio decreases, leading to more ‘noise’ (scatter) in the results. Furthermore, all
496 radiometers have some kind of an internal temperature reference kept at around ambient
497 temperature and often a second reference slightly above this, and therefore have the highest
498 accuracy around these temperatures. The further away the target temperature becomes from
499 ambient, the larger the extrapolation from the internal references, and therefore the larger the
500 uncertainty. Finally, the BBs used to calibrate the radiometers, a Landcal P80P or a
501 CASOTS/CASOTS-II, are not equipped with purge systems to prevent formation of dew and
502 frost in the BB cavity. This means that the use of the BBs is limited to above the dew point,
503 which is normally above 0 °C; or, if they are used below the dew point, they could be
504 affected by dew and frost. The participant scales in the temperature range to below 0 °C are
505 therefore most likely realized by extrapolation, leading to increased uncertainty at these
506 temperatures.

507 Even though a lower target temperature introduces various difficulties for accurate
508 temperature measurement the declared uncertainties do not increase as expected, and for
509 some participants they are almost the same as in the ambient temperature range. In the
510 temperature range below 0 °C, the error bars of the measurements do not necessarily overlap
511 with that of the reference, indicating that the uncertainty estimation does not fully represent
512 the true measurement capabilities of the participants. The result suggests that all participants
513 need to reconsider the uncertainty budget so that such effects as extrapolation from the
514 calibration temperature, low signal level due to reduced radiance, and larger deviation of the
515 target temperature from the internal blackbody temperature are adequately taken into account
516 in order that the uncertainties reflect the true measurement capabilities.

517 From the point of view of SST_{skin} retrieval, increasing the uncertainty is not an issue,
518 since measurement at these low temperatures is required only for measurement of the sky
519 brightness temperature and not for the sea surface brightness temperature. Sky brightness
520 temperature is used in the correction for reflection at the sea surface when deriving the
521 SST_{skin} from the sea surface brightness temperature. Since the emissivity of the sea surface is
522 high, this correction is small especially when the sky has no overcast cloud and its brightness
523 temperature is low. For instance, sky brightness temperature measurement error of 10 K at –
524 30 °C will only introduce an error of around 50 mK in the derived SST_{skin}. Thus the
525 requirement for accuracy in the sky brightness temperature is much more relaxed.

526 **9. Conclusion**

527 Six SST_{skin} retrieval radiometers as well as five BBs used for calibrating them were
528 gathered at NPL and their realised brightness temperatures were compared against the NPL
529 reference standard scale as a part of the CEOS International Thermal Infrared Radiometer
530 Inter-comparison (CRIC). During the comparison which took place during five days in June
531 2022, the BBs were measured with the transfer standard radiometer calibrated against the
532 reference standard radiometer, AMBER, on which the scale was realised radiometrically
533 traceable to the ITS-90 primary standards of NPL. The six radiometers viewed the cavities of
534 an NH3-BB and a SL-BB, and brightness temperatures detected by the radiometers were
535 compared against the values derived from the platinum resistance thermometers measuring
536 the BBs, which were calibrated traceable to the ITS-90 primary standards of NPL.

537 The temperature range of the BB comparison covered from 10 °C to 35 °C for all
538 participants, and to 50 °C for two of the participants. The brightness temperature reported by
539 the participants agreed with the reference value measured by the NPL transfer standard
540 radiometer within the uncertainties for all temperatures and for all BBs.

541 The SL-BB was applied for comparison in the range 0 °C to 30 °C. The temperature
542 range of most interest from the SST_{skin} retrieval point of view is 10 °C to 30 °C, and in this
543 temperature range all participants reported results that were in good agreement with the
544 reference.

545 The NH3-BB was applied to the extreme temperatures at –30 °C, –15 °C, 0 °C, 30 °C, 35
546 °C, 40 °C, and 50 °C. The temperatures above 30 °C showed good agreement, similar to 30
547 °C. On the other hand, at and below 0 °C, the participant reported values showed divergence

548 from the reference which grew as the temperature became lower, and the divergence
549 exceeded the uncertainties. This will not have a major significance in the derivation of the
550 SST_{skin}, since this low temperature range is only required for sky brightness temperature
551 measurement, is used for correction of the reflection at sea surface, and this requires lower
552 accuracy. However, it indicates there is deficiency in the uncertainty estimation capability for
553 all participants, especially when the derived SST_{skin} deviates from the ambient, and this
554 should be improved in future if the participants are to maintain confidence in their SST_{skin}
555 retrieval capabilities.

556 Three new features were introduced in the current comparison compared to the previous
557 comparison in 2016. The first is the introduction of the transfer standard radiometer to
558 perform the measurement of the BBs. This overcomes the issue of the short-term stability of
559 the AMBER, eliminates the thermal interaction of the cryogenically cooled AMBER with the
560 BB, and reduces the problem with its poor operability encountered during practical
561 measurements. The second is the employment of a novel scale realisation on the AMBER
562 utilising two reference temperatures, which resulted in reduced uncertainty and made the
563 realisation of a zero-radiance source unnecessary. The third is the introduction of the new SL-
564 BB. This proved to have a positive impact, not only for improved efficiency of the
565 measurements, but also from the point of view of improvement in measurement accuracy by
566 the participants owing to its large aperture, high emissivity, and temporal stability.
567 Measurement of the two BBs made at same temperatures showed similar agreement, which
568 confirmed that they produce identical comparison results.

569 It should also be noted that the comparison in the laboratory is not always equivalent to
570 measurement in the field. The comparison results show that divergence from the reference is
571 noticeable where the target temperature diverts from the ambient temperature. The
572 instruments tested here utilise internal reference BBs at temperatures at around the ambient,
573 which means high accuracy is expected if the target is around the ambient. In the laboratory,
574 this is not always the case, for the room temperature is maintained around 23 °C regardless of
575 the BB source temperature. On the other hand, in the field the ambient temperature is nearly
576 always close to the SST_{skin}. Performance of the instruments when deriving SST_{skin} should
577 therefore be expected to be better in practice compared to what this comparison shows, and
578 the results shown in this comparison should be interpreted as a worst-case scenario. The

579 result of the accompanying field comparison shows very good agreement among participants,
580 and this seems to support the above observation (Yamada et al. 2023c; 2023d).

581 In recent years, new improved radiometers for SST_{skin} retrieval have been developed, and
582 more radiometers are being deployed at the sea. A future repeat of the current comparison
583 exercise will be needed, possibly with a reduced interval between comparisons than the
584 current six to eight years, when the new radiometers are being used in the field.

585

586 *Acknowledgments.*

587 This work was funded by the ESA contract FRM4SST Phase II. The UoV participants
588 took part in the comparison with the support of the research projects PID2020-118797RBI00
589 (MCIN/AEI/10.13039/501100011033) and PROMETEO/2021/016 (Generalitat Valenciana).

590

591 *Data Availability Statement.*

592 Datasets for this research are included in Yamada et al. (2023a, 2023b) at the following.

593 [https://ships4sst.org/sites/shipborne-radiometer/files/documents/FRM4SST-CRICR-NPL-](https://ships4sst.org/sites/shipborne-radiometer/files/documents/FRM4SST-CRICR-NPL-001_ISSUE-1.pdf)
594 001_ISSUE-1.pdf

595 [https://ships4sst.org/sites/shipborne-radiometer/files/documents/FRM4SST-CRICR-NPL-](https://ships4sst.org/sites/shipborne-radiometer/files/documents/FRM4SST-CRICR-NPL-002_ISSUE-1.pdf)
596 002_ISSUE-1.pdf

597

REFERENCES

598 Barker-Snook, I., Theocharous, E. and Fox, N. P., 2017a: *2016 comparison of IR brightness*
599 *temperature measurements in support of satellite validation. Part 2: Laboratory*
600 *comparison of radiation thermometers, NPL Report ENV 14*, [http://www.frm4sts.org/wp-](http://www.frm4sts.org/wp-content/uploads/sites/3/2017/12/FRM4STS_D100_TR-2_Part2_Radiometer_23Jun17-signed.pdf)
601 [content/uploads/sites/3/2017/12/FRM4STS_D100_TR-2_Part2_Radiometer_23Jun17-](http://www.frm4sts.org/wp-content/uploads/sites/3/2017/12/FRM4STS_D100_TR-2_Part2_Radiometer_23Jun17-signed.pdf)
602 signed.pdf

603 Barker-Snook, I., Theocharous, E. and Fox, N. P., 2017b: *2016 comparison of IR brightness*
604 *temperature measurements in support of satellite validation. Part 3: Sea surface*
605 *temperature comparison of radiation thermometers, NPL Report ENV 15*,
606 [http://www.frm4sts.org/wp-content/uploads/sites/3/2017/12/FRM4STS_D100_TR-](http://www.frm4sts.org/wp-content/uploads/sites/3/2017/12/FRM4STS_D100_TR-2_Part3_WST_23Jun17-signed.pdf)
607 [2_Part3_WST_23Jun17-signed.pdf](http://www.frm4sts.org/wp-content/uploads/sites/3/2017/12/FRM4STS_D100_TR-2_Part3_WST_23Jun17-signed.pdf)

608 Barton, I. J., Minnett, P. J., Maillet K. A., Donlon, C. J., Hook, S. J., Jessup, A. T. and
609 Nightingale, T.J., 2004: The Miami 2001 infrared radiometer calibration and
610 intercomparison: Part II Shipboard results *J. Atmos. Ocean Techn.* **21**, 268-283.

611 Bloembergen, P., 1999: On the correction for the size-of-source effect corrupted by
612 background radiation *Proceedings of TEMPMEKO '99, Seventh International Symposium*
613 *on Temperature and Thermal Measurements in Industry and Science*, J F Dubbeldam and
614 M J de Groot eds., IMEKO/NMi Van Swinden Laboratorium, 607–612

615 Bojinski, S., Verstraete, M., Peterson, T. C., Richter, C., Simmons, A. and Zemp, M., 2014:
616 The concept of essential climate variables in support of climate research, applications,
617 and policy *Bull. Amer. Meteor. Soc.* **95**, 1431–1443.

618 Chu, B. and Machin, G., 1999: A low-temperature blackbody reference source to $-40\text{ }^{\circ}\text{C}$
619 *Meas. Sci. Technol.* **10**, 1-6.

620 Donlon, C. J., Nightingale, T., Fiedler, L., Fisher, G., Baldwin, D. and Robinson, I. S., 1999:
621 The Calibration and Intercalibration of Sea-Going Infrared Radiometer Systems Using a
622 Low Cost Blackbody Cavity *J. Atmos. Ocean Techn.* **16**, 1183-1197

623 Donlon, C., Robinson, I. S., Wimmer, W., Fisher, G., Reynolds, M., Edwards, R. and
624 Nightingale, T. J., 2008: An infrared sea surface temperature autonomous radiometer
625 (ISAR) for deployment aboard volunteer observing ships (VOS) *J. Atmos. Ocean Techn.*,
626 **25**, 93-113.

627 Donlon, C., Wimmer, W., Robinson, I. S., Fisher, G., Ferlet, M., Nightingale, T. J. and Bras,
628 B., 2014: A Second-Generation BB System for the Calibration and Verification of
629 Seagoing Infrared Radiometers *J. Atmos. Ocean Techn.*, **31**, 1104-1127

630 Donlon, C., Berruti, B., Buongiorno, A., Ferreira, M.-H., Féménias, P., Frerick J., Goryl P.,
631 Klein U., 2012: The Global Monitoring for Environment and Security (GMES) Sentinel-3
632 mission *Remote Sensing of Environment*, **120**, 37-57

633 Gutschwager, B., Theocharous, E., Monte, C, Adibekyan, A., Reiniger, M., Fox, N. P. and
634 Hollandt, J., 2013: Comparison of the radiation temperature scales of the PTB and the
635 NPL in the temperature range from $-57\text{ }^{\circ}\text{C}$ to $50\text{ }^{\circ}\text{C}$ *Meas. Sci. Technol.* **24** 065002 (9pp)

636 Machin, G. and Chu, B., 1998: A transportable gallium melting point BB for radiation
637 thermometry calibration *Meas. Sci. Technol.*, **9**, 1653–1656

638 McEvoy, H. and Simpson, R. and Korniliou, S., 2024: NPL large aperture, low temperature
639 blackbody source for improved calibration of wide field-of-view instruments, in
640 preparation

641 Minnett, P. J. and Barton I. J., 2010: Chapt. 6. Remote Sensing of the Earth's Surface
642 Temperature *Radiometric Temperature Measurements II. Applications*, Z. M. Zhang, et
643 al., eds., Elsevier Inc., 334.

644 Ohring, G., Wielicki, B., Spencer, R., Emery, B., Datla, R., 2005: Satellite instrument
645 calibration for measuring global climate change: report of a workshop. *Bull. Am.*
646 *Meteorol. Soc.*, **86**, 1303–1313.

647 Preston-Thomas, H., 1990: The International Temperature Scale of 1990 (ITS-90) *Metrologia*
648 **27**, 3-10.

649 Rice, J. P., Butler, J. I., Johnson, B. C., Minnett, P. J., Maillet K. A., Nightingale, T. J, Hook,
650 S. J., Abtahi, A., Donlon, C. J. and. Barton, I. J., 2004: The Miami 2001 infrared
651 radiometer calibration and intercomparison. Part I: Laboratory characterisation of BB
652 targets *J. Atmos. Ocean Techn.*, **21**, 258-267.

653 Theocharous, E., Fox, N. P., Sapritsky, V. I., Mekhontsev, S. N. and Morozova, S. P., 1998:
654 Absolute measurements of black-body emitted radiance *Metrologia* **35**, 549-554

655 Theocharous, E. and Fox, N. P., 2010: *CEOS comparison of IR brightness temperature*
656 *measurements in support of satellite validation. Part II: Laboratory comparison of the*
657 *brightness temperature of BBs, NPL Report COM OP4*,
658 <https://eprintspublications.npl.co.uk/4759/>

659 Theocharous, E., Usadi, E. and Fox, N. P., 2010: *CEOS comparison of IR brightness*
660 *temperature measurements in support of satellite validation. Part I: Laboratory and*
661 *ocean surface temperature comparison of radiation thermometers, NPL Report COM*
662 *OP3*, <http://eprintspublications.npl.co.uk/4744/>

663 Theocharous, E., Barker-Snook, I. and Fox, N. P., 2017: *2016 comparison of IR brightness*
664 *temperature measurements in support of satellite validation. Part 1: Laboratory*
665 *comparison of the brightness temperature of BBs, NPL Report ENV 12*,
666 [http://www.frm4sts.org/wp-content/uploads/sites/3/2017/12/FRM4STS_D100_TR-](http://www.frm4sts.org/wp-content/uploads/sites/3/2017/12/FRM4STS_D100_TR-2_Part1_Blackbody_23Jun17-signed.pdf)
667 [2_Part1_Blackbody_23Jun17-signed.pdf](http://www.frm4sts.org/wp-content/uploads/sites/3/2017/12/FRM4STS_D100_TR-2_Part1_Blackbody_23Jun17-signed.pdf)

668 Theocharous, E., Fox, N. P., Barker-Snook, I., Niclòs, R., García-Santos, V., Minnett, P. J.,
669 Göttsche, F. M., Poutier, L., Morgan, N., Nightingale, T., Wimmer, W., Høyer, J., Zhang,
670 K., Yang, M., Guan, L., Arbelo, M. and Donlon, C. J., 2019: The 2016 CEOS infrared
671 radiometer comparison: Part 2: Laboratory comparison of radiation thermometers, *J.*
672 *Atmos. Ocean Techn.*, **36**, 1079-1092.

673 WMO, 2022: *The 2022 GCOS Implementation Plan (GCOS-244)*,
674 https://library.wmo.int/doc_num.php?explnum_id=11317

675 Yamada, Y. and Fox, N., 2022: *Fiducial Reference Measurements for Sea Surface*
676 *Temperature (FRM4SST): Protocol for FRM4SST CRIC Laboratory Comparison of*
677 *Radiometers and Blackbodies*, [https://ships4sst.org/sites/shipborne-](https://ships4sst.org/sites/shipborne-radiometer/files/documents/FRM4SST-CRICR-NPL-001_ISSUE-1.pdf)
678 [radiometer/files/documents/FRM4SST-CRICR-NPL-001_ISSUE-1.pdf](https://ships4sst.org/sites/shipborne-radiometer/files/documents/FRM4SST-CRICR-NPL-001_ISSUE-1.pdf)

679 Yamada, Y., Harris, S., Wimmer, W., Holmes, R., Nightingale, T., Lee, A., Morgan, N.,
680 Göttsche, F.-M., Niclòs, R., Perelló, M., Donlon, C. and Fox, N., 2023a: *Fiducial*
681 *Reference Measurements for Sea Surface Temperature (FRM4SST): D90 – Results from*
682 *CEOS International Thermal Infrared Radiometer Inter-comparison (CRIC), Part 1 of 3:*
683 *Laboratory Comparison of Blackbodies*, [https://ships4sst.org/sites/shipborne-](https://ships4sst.org/sites/shipborne-radiometer/files/documents/FRM4SST-CRICR-NPL-001_ISSUE-1.pdf)
684 [radiometer/files/documents/FRM4SST-CRICR-NPL-001_ISSUE-1.pdf](https://ships4sst.org/sites/shipborne-radiometer/files/documents/FRM4SST-CRICR-NPL-001_ISSUE-1.pdf)

685 Yamada, Y., Harris, S., Hayes, M., Simpson, R., Wimmer, W., Holmes, R., Nightingale, T.,
686 Lee, A., Jepsen, N., Morgan, N., Göttsche, F.-M., Niclòs, R., Perelló, M., Donlon, C. and
687 Fox, N., 2023b: *Fiducial Reference Measurements for Sea Surface Temperature*
688 *(FRM4SST): D90 – Results from CEOS International Thermal Infrared Radiometer Inter-*
689 *comparison (CRIC), Part 2 of 3: Laboratory Comparison of Radiometers*,
690 [https://ships4sst.org/sites/shipborne-radiometer/files/documents/FRM4SST-CRICR-NPL-](https://ships4sst.org/sites/shipborne-radiometer/files/documents/FRM4SST-CRICR-NPL-002_ISSUE-1.pdf)
691 [002_ISSUE-1.pdf](https://ships4sst.org/sites/shipborne-radiometer/files/documents/FRM4SST-CRICR-NPL-002_ISSUE-1.pdf)

692 Yamada, Y., Harris, S., Wimmer, W., Holmes, R., Nightingale, T., Lee, A., Jepsen, N.,
693 Morgan, N., Göttsche, F.-M., Niclòs, R., Perelló, M., Garcia-Santos, V., Donlon, C. and
694 Fox, N., 2023c: *Fiducial Reference Measurements for Sea Surface Temperature*
695 *(FRM4SST): D90 – Results from CEOS International Thermal Infrared Radiometer Inter-*
696 *comparison (CRIC), Part 3 of 3: Field Comparison of Radiometers*,
697 [https://ships4sst.org/sites/shipborne-radiometer/files/documents/FRM4SST-CRICR-NPL-](https://ships4sst.org/sites/shipborne-radiometer/files/documents/FRM4SST-CRICR-NPL-003_ISSUE-1.pdf)
698 [003_ISSUE-1.pdf](https://ships4sst.org/sites/shipborne-radiometer/files/documents/FRM4SST-CRICR-NPL-003_ISSUE-1.pdf)

699 Yamada, Y., Harris, S., Wimmer, W., Holmes, R., Nightingale, T., Lee, A., Jepsen, N.,
700 Morgan, N., Göttsche, F.-M., Niclòs, R., Perelló, M., Garcia-Santos, V., Donlon, C. and
701 Fox, N., 2023d: 2022 CEOS International Thermal Infrared Radiometer Comparison: Part
702 II: Field Comparison of Radiometers, submitted to *J. Atmos. Ocean Techn.*

703 Yamada, Y., Harris, S., Theocharous, E. and Hayes, M., 2023e: A novel radiometric
704 calibration of an infrared thermometer *Metrologia* **60**, 065005 (8pp)
705 <https://doi.org/10.1088/1681-7575/acffcb>